Rate enhancement of the catechol oxidase activity of a series of biomimetic monocopper(II) complexes by introduction of non-coordinating groups in N-tripodal ligands

Ronan Marion, Nidal Saleh, Nicolas Le Poul, Didier Floner, Olivier Lavastre, Florence Geneste

NJC

Cite this: *New J. Chem.*, 2012, **36**, 1828–1835

www.rsc.org/njc

PAPER

Rate enhancement of the catechol oxidase activity of a series of biomimetic monocopper(II) complexes by introduction of non-coordinating groups in *N*-tripodal ligands†

Ronan Marion,[a] Nidal M. Saleh,[a] Nicolas Le Poul,[b] Didier Floner,[a] Olivier Lavastre[c] and Florence Geneste*[a]

Received (in Montpellier, France) 6th April 2012, Accepted 13th June 2012
DOI: 10.1039/c2nj40265c

Asymmetrical *N*-tripodal ligands have been synthesized in three steps. Diversity has been introduced at the first step of the synthesis by adding pyrazine, pyridine, benzyl and thiophene rings. The corresponding Cu^{II} complexes have been prepared by reaction with $CuCl_2$ and characterized by Electron Paramagnetic Resonance (EPR), UV-Vis spectroscopies and cyclic voltammetry. The data show that the ligand coordinates to Cu^{II} in a mononuclear fashion in solution and that the complexes display a square pyramidal geometry. All complexes are characterized by a quasi-reversible one-electron redox behavior in acetonitrile. The ability of the complexes to oxidize 3,5-di-*tert*-butylcatechol to 3,5-di-*tert*-butylquinone has been studied and the results show that the rate of the reaction depends on the basicity and the steric hindrance of the heterocyclic donor. Best results have been obtained with Cu^{II} complexes coordinated to bidentate ligands, since they facilitate the approach and the coordination of catechol to the metal. Particularly, the introduction of a thiophenyl group to mimic the sulfur atom at proximity to the catalytic center in the catechol oxidase protein structure improves the catalytic activity of the complex.

Introduction

Catechol oxidase (CO) is a copper-containing protein with a type-3 active site, consisting of two closely spaced copper ions each coordinated by three histidine residues. Like other type-3 copper proteins, such as hemocyanin and tyrosinase, it has the ability to reversibly bind and activate dioxygen. Whereas hemocyanin is an oxygen transport storage protein and tyrosinase catalyzes the orthohydroxylation of phenols with further oxidation of the catechol product to the *o*-quinone, CO lacks hydroxylase activity, but catalyzes the oxidation of *o*-diphenols to the corresponding *o*-quinones by molecular oxygen reduction with a two-electron reaction for each oxidized *o*-diphenol function. In order to gain insights into the catalytic mechanism of a type-3 dicopper enzyme, structures of the oxidized Cu^{II}–Cu^{II} and the reduced Cu^{I}–Cu^{I} CO forms from sweet potato (*Ipomoea batatas*) were determined by X-ray crystallography.[1] In both structures, the active site is formed by two copper centers, each coordinated by three imidazoles from the histidine residues (Fig. 1).

In the oxidized CO state, the two Cu^{II} centers contain a hydroxide bridging group completing the four-coordinated trigonal pyramidal coordination sphere, and the Cu^{II}–Cu^{II} distance was determined to be 2.9 Å. Upon reduction of the enzyme the metal–metal separation increases significantly to 4.4 Å. An interesting feature of the dinuclear metal center in catechol oxidase is the covalent thioether bond existing between one of the three histidine residues coordinated to Cu_A (His 109) and one non-coordinating cysteine (Cys 92). Such thioether bonds were also detected in several tyrosinase and hemocyanin[2–4] active sites, but not systematically.[5–8] The fine analysis of the structures suggested that the presence of the

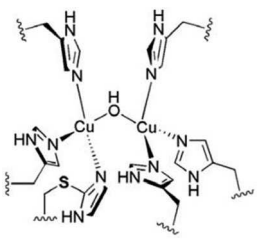

Fig. 1 The active site of catechol oxidase.

[a] *Université de Rennes 1, UMR-CNRS 6226, Laboratoire des Sciences Chimiques de Rennes, Equipe Matière Condensée et Systèmes Electroactifs, Campus de Beaulieu, 35042 Rennes cedex, France. E-mail: florence.geneste@univ-rennes1.fr; Fax: +33 2 23 23 59 67*
[b] *Laboratoire de Chimie, Electrochimie Moléculaires et Chimie Analytique, CNRS, UMR 6521, Université Européenne de Bretagne à Brest, 6 av. Le Gorgeu, 29238 Brest cedex, France*
[c] *Université de Rennes 1, UMR-CNRS 6164, Institut d'Electronique et Télécommunications de Rennes, Campus de Beaulieu, 35042 Rennes cedex, France*

† Electronic supplementary information (ESI) available: NMR and spectroscopic data. See DOI: 10.1039/c2nj40265c

thioether induces geometric effects, which constrain the Cu_A center in a trigonal conformation, thus enhancing electron transfer kinetics by an increase of the reduction potential. Also, it has been shown that this group induces conformational stabilization at the active site, leading to a fixed orientation of the histidine that is optimal for further coordination of the Cu_A atom.[9]

The investigation of the catecholase activity of molecular copper complexes is a convenient method to detect functional mimics of oxygenases and oxidases, or new catalysts for oxidation reactions. Dinuclear models of catechol oxidase with Cu–Cu distance <5 Å have proved their efficiency. Most of them were symmetrical with coordinating groups (pyridine, imidazole, pyrazole...) mimicking the three imidazole donors from the histidine residues.[10–15] Some asymmetrical dicopper complexes have also been prepared.[16–23] One evoked reason was to "open" coordination sites to improve the interaction of the metal center with the substrate. Interestingly, the resulting catalytic properties were shown to be enhanced when such asymmetry was created. For instance, the study of a bis-Cu complex with an amino group and two pyridines coordinated on one side, and two nitrogen atoms from pyridine on the other side has shown a high rate for the catalysis of catechol.[20] Another reason was to model the asymmetric feature of catechol oxidase due to the presence of the uncoordinating thioether bond on one of the coordinated histidine residues as mentioned previously. To our knowledge, there exists only one example of a asymmetric dinuclear complex with a thioether group.[19] For this complex, DFT calculations and ESI-MS experiments showed that the sulfur atom from the thioether was coordinated to the metal ion in solution. An alternative strategy was developed by using a weak thiophene donor group to model the thioether and prevent coordination to Cu^{II}, as it occurs in type 3 copper proteins.[24–26] However, poor catecholase activity was reported for copper(II) complexes bearing a bis-thiophene ligand. Also the role of the thiophene groups in the catalytic reaction was not evoked.[24] The beneficial presence of the thiophene substituent was only highlighted in catalytic polymerization of 2,6-dimethylphenol, attributed to the stabilization of copper(I) species in the catalytic cycle.[25]

Many simple mononuclear complexes have also been studied and have shown good catecholase activities.[27–40] However, a few examples of monocopper complexes with sulfur atoms have been described in the literature.[41,42] They were mainly designed to tune the geometry through forced coordination of thioether groups, thus enhancing electron transfer properties. Despite the fact that they are drifted from modeling biological systems, mononuclear complexes are interesting because their synthesis is easier and allows the modification of their structure in a systematic way, providing a better understanding of the elements favoring their catecholase activity. Thus, we previously prepared monocopper complexes based on bis-pyrazolyl *N*-tripodal ligands containing a functionalized chain.[43] The variety, introduced both on the substituents of the pyrazole ring and on the side chain, allowed us to rationalize the effect of the oxygen atom in the third position of the side chain and the electronic and steric effects of substituents on pyrazole rings.

In our effort to develop efficient mononuclear catalysts and study their structure–activity relationship, we have prepared a new series of mononuclear complexes based on asymmetrical *N*-tripodal ligands with a pyrazole group on one arm and pyridine, pyrazine, phenyl or thiophenyl ring on the second arm, the hexanol chain being still present on the third branch for further applications in supported catalysis.[44] The thiophenyl substituent has been chosen to add an uncoordinating sulfur atom in the complex structure, in an attempt to mimic the effect of the thioether bond present in catechol oxidase by geometric and electronic modifications. Moreover, since it is smaller than the phenyl group, it is expected to facilitate the coordination of the catechol substrate to the Cu(II) center. We report here the synthesis, UV, EPR, electrochemical characterization, and catecholase activity study of these new Cu^{II} complexes.

Results

Synthesis of complexes

The synthesis of unsymmetrical *N*-tripodal ligands was achieved in three steps (Scheme 1).

The first step consists of the condensation reaction of 6-aminohexan-1-ol with aldehydes **1a–d** to give an imine intermediate. After reduction with $NaBH_4$, the obtained amino compounds **2a–d** were condensed with 1-hydroxymethylpyrazole at 70 °C for 3 h without solvent to give the asymmetrical *N*-tripodal ligands **3a–d**. To avoid the presence of remaining amino compounds **2a–d** that could form a complex with $CuCl_2$, 10% excess of 1-hydroxymethylpyrazole was necessary in the last step of the synthesis. As shown by ^{1}H-NMR analysis, under these conditions, the asymmetrical *N*-tripodal ligand was obtained without remaining amino compounds **2a–d**. The products were used without further purification for the complexation reaction. Copper complexes were formed by reaction with $CuCl_2$ in anhydrous tetrahydrofuran at room temperature for 2 h. They were isolated by precipitation and then characterized in their more stable monohydrated form.

Spectroscopic characterization

The mononuclear complexes were analyzed by electronic absorption spectroscopy in methanol, showing a wide visible

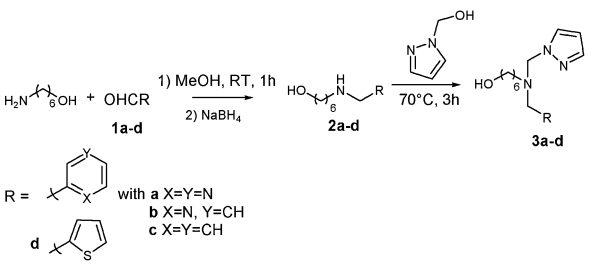

Ligand	3a	3b	3c	3d	3e
Complex	4a	4b	4c	4d	4e[a]

[a] previously prepared by a condensation reaction between 1-hydroxymethylpyrazole and 6-aminohexan-1-ol[43]

Scheme 1

Table 1 UV-Vis absorption data and EPR spectral data for copper(II) complexes **4a–e**

Complex	UV-Vis[a] (λ_{max}/nm) (ε/M^{-1} cm^{-1})	EPR[b] $g_{\|}$	$g_{\perp}$	$A_{\|}$[c]
4a	705 (153)	2.21	2.11	180
4b	685 (137)	2.22	2.05	173
4c	741 (83)	2.39	2.09	155
4d	750 (70)	2.39	2.09	142
4e[43]	705 (145)	2.23	2.06	166

[a] CH_3OH solution of 10^{-2} mol L^{-1} metal complex at 298 K. [b] Frozen CH_3OH solution of 10^{-2} mol L^{-1} metal complex at 69 K. [c] Hyperfine coupling constant, $A_{\|}/10^{-4}$ cm^{-1}.

absorption band in the region of d–d transitions at 685–750 nm (ε = 70–153 M^{-1} cm^{-1}) (Table 1). This wavelength range is indicative of a d–d electronic transition for Cu complexes in a square-based pyramidal (SBP) conformation (bipyramid trigonal complexes (BPT) are usually characterized by a λ_{max} of 850 nm).[45]

The absorption wavelengths are red shifted with copper complexes **4c** and **4d**, as a result of distorted geometry and/or change of the primary environment (coordination of MeOH).

The EPR spectra of complexes **4a–d** were recorded at 69 K in frozen methanol (Table 1). All complexes display an EPR axial signal, which is typical of a mononuclear Cu^{II} complex in a square-based pyramidal geometry ($g_{\|} > g_{\perp}$), confirming UV-Vis predictions. The half-field splitting signal, usually observed for dinuclear species in the solid state, was not detected for these complexes, emphasizing the predominance of mononuclear species in solution, as previously observed with bis(pyrazole) analogous complexes.[43] The parallel hyperfine coupling between the unpaired electron and the copper nuclear spins ($A_{\|}$) was determined for each species by spectrum simulation (Table 1). For complexes **4a** and **4b**, the parameters are fully consistent with a Cu complex with SBP geometry and surrounded by a nitrogen ligand and belong to the Peisach–Blumberg assumptions:[46,47] $g_{\|}$ = 2.21 and $A_{\|}$ = 173–180 × 10^{-4} cm^{-1}. With **4c** and **4d** complexes, the $g_{||}$ value is significantly higher whereas $A_{\|}$ is lower. These discrepancies can be correlated to the UV-Vis data and interpreted as the coordination of one MeOH ligand to Cu(II): this induces a slight change of the geometry and/or a decrease of the electronic intensity on Cu(II). This last hypothesis is consistent with Peisach–Blumberg assumptions considering the substitution of N-donor by O-donor ligands ($g_{\|}$ = 2.40 and $A_{\|}$ = 130 G values for a Cu center with 4 oxygen ligands).

Electrochemical properties

Cyclic voltammetry of the complexes was performed on a glassy carbon electrode in CH_3CN–NBu_4PF_6 and CH_2Cl_2–NBu_4PF_6 at v = 0.1 V s^{-1} (Fig. 2). Data are summarized in Table 2.

Quasi-reversible systems corresponding to the $Cu^{II/I}$ couple were obtained in acetonitrile, with peak separation (ΔE_p) ranging from 0.11 to 0.26 V and a ratio of anodic to cathodic currents (i_{pa}/i_{pc}) between 0.9 and 1.1. The average of the peak potentials was taken as an approximation of the formal potential ($E_{1/2}$). For complexes **4a** and **4b**, the potential value ($E_{1/2}$) is fully dependent on the basicity of the heterocycle: **4b** < **4a**. Indeed, the donor effect of the pyridine ring (pK_a = 5.2) is clearly

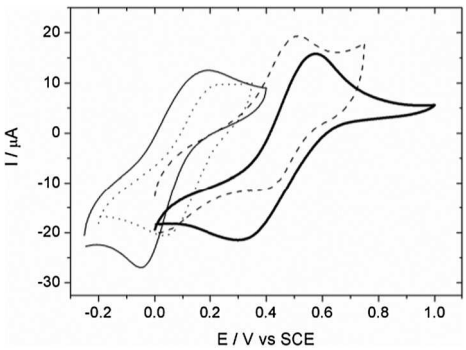

Fig. 2 Cyclic voltammograms of **4a** (···), **4b** (—), **4c** (---) and **4d** (—) in acetonitrile + 0.1 M tBu_4NPF_6. Scan rate 0.1 V s^{-1}.

Table 2 Cyclic voltammetry (E/V *vs.* SCE) data in acetonitrile of copper(II) complexes **4a–e**

Complex	E_{pa}/V	E_{pc}/V	$E_{1/2}$/V	ΔE_p/V	i_{pa}/i_{pc}
4a	0.24	0.03	0.13	0.21	0.9
4b	0.17	−0.04	0.06	0.21	0.9
4c	0.50	0.39	0.44	0.11	1.1
4d	0.57	0.31	0.44	0.26	1.1
4e[43]	0.34	0.20	0.27	0.14	1.0

highlighted by the low potential value of complex **4b**. This effect was less pronounced with pyrazine-containing complex **4a**, since the pK_a of pyrazine is only 0.6. Complexes **4c** and **4d** containing phenyl and thiophenyl groups, respectively, present significantly higher potential values than their tridentate analogues **4a** and **4b** (≈ +0.3 V), due to the absence of coordination between the copper metal and a third donor nitrogen atom. The similar electrochemical behavior of the two complexes tends to show that the thiophenyl ring is not coordinated to the metal in **4d** in agreement with spectroscopic results.

For better knowledge of the species coordinated to the metal in solution, **4c** and **4d** were also analyzed by cyclic voltammetry on a glassy carbon electrode in anhydrous CH_2Cl_2–NBu_4PF_6 at v = 0.1 V s^{-1}. A quasi-reversible system corresponding to the $Cu^{II/I}$ couple was obtained for both complexes, with formal potential values equal to $E_{1/2}$ = 0.50 and 0.32 V_{SCE}, respectively. When a large excess of dry acetonitrile or MeOH was added, the redox potential shifted both to 0.40 V_{SCE}, which is similar to the value found in pure CH_3CN (Table 2). The shift of the potential can thus be explained by the replacement of the initial donor ligands (for example, the OH terminal group of the six carbon chain, and/or a chloride ion) by solvent molecules.

Kinetic studies

The catecholase activity of the copper(II) complexes was studied by testing their ability to catalyze 3,5-di-*tert*-butylcatechol. This substrate with two bulky *tert*-butyl substituents on the ring is highly stable and has a low quinone–catechol reduction potential that makes it easily oxidized to the corresponding *o*-quinone. The kinetics of formation of 3,5-di-*tert*-butylquinone in the presence of complexes **4a–d** was continually monitored using a dipping probe colorimeter, since the quinone presents a strong absorption band at 400 nm. The reaction was performed for 1 h at constant agitation and temperature of 25 °C and with a

Table 3 Catalytic activity of copper(II) complexes **4a–e**

	Without catalyst	**4a**	**4b**	**4c**	**4d**	**4e**[43]
Rate/10^8 mol L^{-1} s^{-1}	0.68	0.44	1.08	1.62	2.89	3.23
Correlation coefficient	0.999	0.998	0.998	0.999	0.997	0.999
Induction time/min	0	15	10	0	20	10

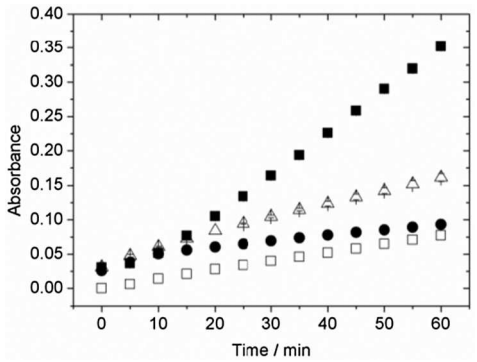

Fig. 3 Plot of absorbance *vs.* time for the oxidation of 3,5-di-*tert*-butylcatechol performed at 25 °C in MeOH without the catalyst □ and catalyzed by **4a** ●, **4b** △, **4e** ■. Error bars are based on two reproducibility measurements.

ratio of a Cu^{II} catalyst over a substrate of 1.5×10^{-3}. These conditions correspond to the beginning of the conversion of catechol into quinone. To compare the catalytic activity of the copper complexes, we determined their rates from the slope of the tangent to the absorbance *versus* time curve after an induction period ranging from 0 to 20 min (Table 3).

Induction periods in catalysis are defined as periods for which the variation of product concentration with time exhibits an inflection point. They are usually observed when the pre-catalyst needs to be transformed into its more active form or when the reaction is auto-catalytic (one of the reactants is also a product). In our case, this induction period has already been observed with symmetrical *N*-tripodal bispyrazolyl copper complexes.[43] As for **4a–d**, structural and spectroscopic analyses have shown that the complexes exist as mononuclear species in solution, whereas X-ray analysis of a symmetrical complex of this family revealed a dinuclear complex with two asymmetrical Cu–Cl–Cu bridges.[48] A spot was considered to be out of the induction period as soon as the correlation coefficient of the best-fit straight line reached 0.997. The kinetic plots for the complexes are given in Fig. 3 and 4.

Discussion

The synthetic method[49] used here led to the preparation of a variety of asymmetrical *N*-tripodal ligands. The systematic comparison of the catecholase activity of the resulting complexes allows a better understanding of the factors influencing their reactivity in the catalytic oxidation of 3,5-di-*tert*-butylcatechol. Particularly, it highlights the influence of the bidentate *vs.* tridentate structure of the ligand on the catalytic properties.

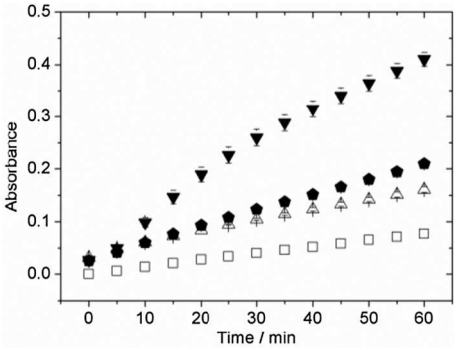

Fig. 4 Plot of absorbance *vs.* time for the oxidation of 3,5-di-*tert*-butylcatechol performed at 25 °C in MeOH without the catalyst □ and catalyzed by **4b** △, **4c** ⬟, **4d** ▽. Error bars are based on two reproducibility measurements.

As previously observed for copper complexes with bis-pyrazolyl *N*-tripodal ligands,[43] the electronic and steric effects of the ligands are known to strongly affect the catalytic activity (Fig. 3). The comparison between Cu complexes **4a** and **4b** is a good indicator of the influence of the basicity of the ligand on the catalytic properties, since both complexes display similar geometries (from EPR/UV-Vis spectroscopies) and steric hindrance. Our studies show that the catecholase catalytic activity of **4b** with a pyridine group is higher than that of **4a** containing a pyrazine ring (Table 3). As previously mentioned, pyridine is a better electron donor than pyrazine. As a consequence, the potential value of **4b** is slightly lower than **4a** (Table 2), meaning that **4b** is more difficult to reduce than **4a**. This indicates that the effectiveness of the whole redox reaction with catechol is correlated to the $E_{1/2}$ of the initial copper complex.

On the basis of such considerations (only basicity effects), compound **4e**[43] containing two pyrazole groups (pK_a = 2.5), and displaying similar geometrical features to **4a** and **4b** (Table 1) should present intermediate catalytic activity and $E_{1/2}$ compared to **4a** and **4b**. However, our studies show that the rate of reaction (**4e** > **4b** > **4a**) follows neither the ligand basicity (**4b** > **4e** > **4a**) nor the potential (**4e** > **4a** > **4b**). Since pyrazole is smaller than pyrazine and pyridine, the enhancement of the oxidation reaction may be due to a decrease of the steric hindrance around the metal, favoring the coordination of catechol.

The oxidation of 3,5-di-*tert*-butylcatechol by complexes coordinated with bidentate nitrogen ligands has been the subject of only a few investigations in the literature, probably due to the fact that the copper ions at the CO active site are coordinated by three imidazoles. Our study gives here the opportunity to directly compare the tridentate *vs.* bidentate design for a better understanding of the role of the tridentate ligand coordinated to the active copper site in the catecholase activity. Our spectroscopic and electrochemical studies have shown that compounds **4c** and **4d** bearing bidentate ligands (**3c** and **3d**) display significant differences with their analogues **4a**, **4b** and **4e**. Indeed, one observes higher redox potential (both anodic and cathodic parts) and remarkable deviation from the typical SBP spectroscopic features obtained with **4a**, **4b** and **4e**. These effects probably result from the absence of coordination of the third arm (phenyl, thiophenyl) of the

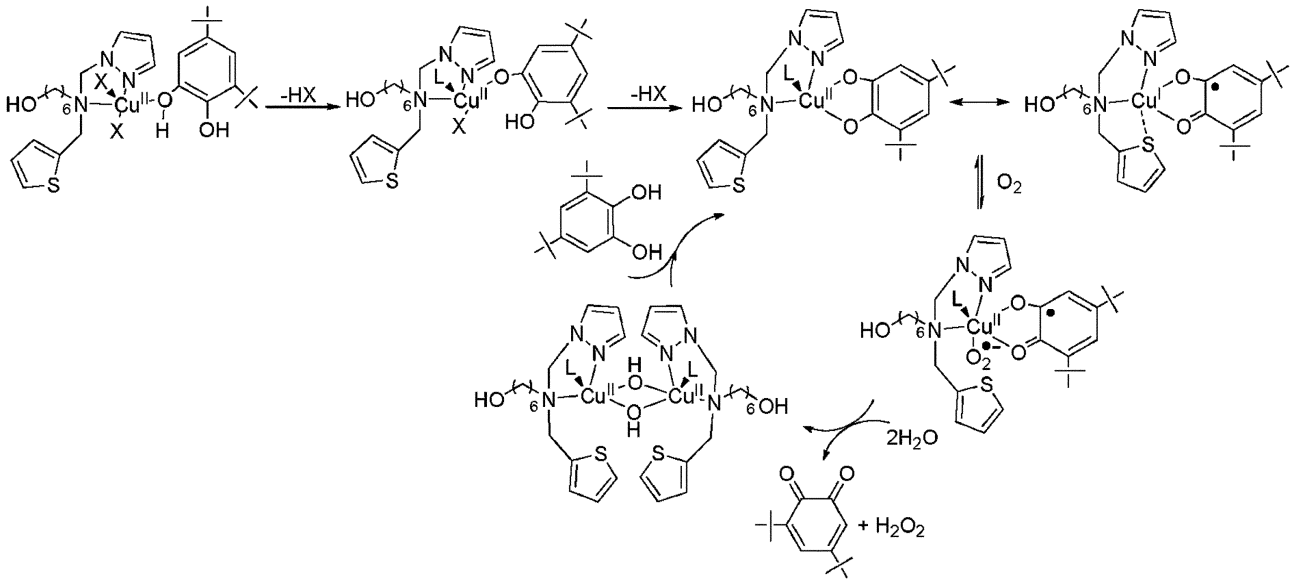

Scheme 2

N-tripodal ligand to the Cu center (partly compensated by solvent coordination), inducing a decrease of the electronic density and geometrical changes, which are kept at both redox states (low peak separation). The properties of the Cu complexes **4c** and **4d** to catalyze the oxidation of 3,5-di-*tert*-butylcathecol were then investigated and compared to their analogues. As shown in Table 3, complex **4c** containing a phenyl group displays a higher catalytic rate for this reaction than **4a** and **4b** bearing pyridine and pyrazine residues with similar steric hindrance (Fig. 4). Two synergetic effects may be responsible for these results for **4c** and **4d**: (i) the lower stability of the Cu^{II} complex due to poor electronic density, and (ii) the higher accessibility of the substrate to the Cu center due to the absence of coordination of one arm. This underlines the interest in using a bidentate ligand to improve the reaction by facilitating the approach and the coordination of catechol to the metal.

Compound **4d** was synthesized in an attempt to mimic the effect of the sulfur atom present in the structure of catechol oxidase and to see if it has an influence on the catalytic activity. Since thiophene is a weak donor group due to electronic delocalization, it can be assumed that it is located close to the catalytic centre without being coordinated to copper, as it occurs for the sulfur atom in the protein structure.

As shown in Table 1 and Fig. 4, **4d** has a better catecholase activity than its analogues **4a–c**. A possible explanation of the improvement in the catecholase activity of **4d** would be the higher accessibility of catechol to the active site as already observed with complex **4c** containing the bidentate ligand **3c**. However the rate obtained with **4d** (2.89×10^{-8} mol L^{-1} s^{-1}) is clearly higher than **4c** (1.62×10^{-8} mol L^{-1} s^{-1}), underlining the interest in adding a thiophenyl group in the asymmetrical complexes structure. Since sulfur-donor compounds are known to be good ligands for low-oxidation-state copper atoms, another explanation for the enhancement of the catalytic activity would be the stabilization of copper(I) species by the thiophene group in the catalytic cycle.[25]

Previous kinetic investigations with **4e** (Scheme 1) based on the Michaelis–Menten model have shown that the catalytic activity of the mononuclear complex characterized by the parameters $k_{cat} = 3.1 \times 10^{-3}$ s^{-1}, $K_M = 1.62$ mM and $k_{cat}/K_M = 1.9$ M^{-1} s^{-1} was significantly lower than those reported for the catalytic oxidation of catechol with CO but was in the range of values found for some dicopper complexes described in the literature.[43] As shown by the rate values depicted in Table 3, the thiophene complex **4d** presents CO activity in the same range as **4e**.

We previously observed with this family of mononuclear copper complexes that dioxygen reduction led to the formation of 1 mole of dihydrogen peroxide for 1 mole of 3,5-di-*tert*-butylquinone and suggested a mechanism based on mononuclear semi-quinonato and a dinuclear bis-μ-hydroxo intermediate.[43] On this basis, we propose here a similar pathway for the catechol oxidation by **4e** (Scheme 2), involving a coordination of the thiophene group by the Cu^{I} intermediate.[25] As demonstrated previously,[50,51] the mechanism involves the formation of copper(I)-semiquinonate intermediate species, which yields, in the presence of dioxygen, the quinone compound and H_2O_2. This mechanism implies also the formation of a reactive superoxo species.

Here, only one molecule of catechol is being oxidized per catalytic cycle, in contrast to the mechanism proposed for the natural enzyme.[1]

Conclusion

In conclusion, a family of asymmetrical copper complexes containing pyrazole ligands was prepared. According to EPR analyses, the complexes mostly exist in solution as mononuclear species and present a square pyramidal geometry. Their catalytic activity toward the oxidation of 3,5-di-*tert*-butylcatechol was compared, allowing us to conclude the structural effects of the ligand on catalysis. First, the comparison of similar copper complexes containing either pyrazine or pyridine rings underlined the importance of the electronic effect of the ligand coordinated to

the metal. Thus a less electron-donating group such as pyrazine enhanced the catalytic activity of the complex, probably favoring the reduction of Cu^{II} into Cu^{I} that occurs in the beginning of the catalytic cycle. Second, the presence of a bulkier coordinating group in the *N*-tripodal ligand (here a pyrazine group compared with a pyrazole group) decreased the kinetic rate, preventing the approach of catechol to the metal. This effect was even more pronounced when a bidentate ligand was used, since it "opens" coordinating sites on the metal. Interestingly, the incorporation of a thiophenyl group in the copper complex structure also significantly enhanced the catalytic activity of the complex, underlining the importance of the presence of a sulfur atom close to the catalytic center. A possible explanation is the stabilization by the thiophene group of copper(I) intermediates in the catalytic cycle.

Experimental section

Materials

Tetrahydrofuran (THF) was distilled from deep blue solutions of sodium–benzophenone ketyl prior to use. All commercially available reagents were used as supplied. Pyrazol-1-yl-methanol[52] and pyrazine-2-carbaldehyde[53] were prepared according to the literature.

Methods

Copper complexes were prepared using Schlenk techniques under an Ar atmosphere. NMR spectra were recorded on a Bruker DPX-200 or a Bruker AH300 FT spectrometer. Chemical shifts are expressed in parts per million downfield from TMS. High resolution mass spectra (HRMS) were obtained with a Waters Q-TOF 2 with an Electrospray Ionisation (ESI) at the Centre de Mesures Physiques de l'Ouest (CRMPO) from Rennes. UV-vis absorption spectra were recorded using a UVIKON 942 spectrophotometer using quartz cuvettes of 1 cm path length. Voltammetric experiments were carried out using an EDAQ potentiostat unit, with the EChem software package. A vitreous carbon working electrode, a platinum wire auxiliary electrode, and a Saturated Calomel reference Electrode (SCE) were used in a standard three-electrode configuration. Cyclic voltammetry analyses were performed in acetonitrile containing 0.1 M tetrabutylammonium hexafluorophosphate, at a 100 mV s^{-1} scan rate, under a dinitrogen atmosphere. EPR spectra were recorded on a Bruker EMX-8/2.7 (X-band) spectrometer at 69 K, and simulated by using the Simfonia© software (Bruker).

Synthesis

6-((Pyrazin-2-ylmethyl)amino)hexan-1-ol (2a). Pyrazine-2-carbaldehyde **1a** (0.92 g, 9 mmol) was added dropwise to 6-aminohexan-1-ol (1 g, 9 mmol) dissolved in methanol (20 mL). The mixture was stirred at room temperature in the presence of $MgSO_4$ for 1 h and then filtered. To the filtrate was added sodium borohydride (0.48 g, 13 mmol) in portions at 0 °C. The mixture was stirred at room temperature for 1 h and then, methanol was evaporated. The resulting residue was dissolved in ether (50 mL) and water (50 mL) was added. The aqueous phase was extracted, the organic phase washed with water (2 × 50 mL) and dried with $MgSO_4$. Filtration and evaporation of the solvent made it possible to obtain the product (1.50 g, 85%) as a yellow oil without further purification. ^{1}H NMR (200 MHz, $CDCl_3$) δ (ppm): 8.63 (s, 1H); 8.54 (d, J = 2.5 Hz, 1H); 8.49 (d, J = 2.5 Hz, 1H); 3.98 (s, 2H); 3.66 (t, J = 6.6 Hz, 2H); 2.70 (t, J = 6.6 Hz, 2H); 1.75 (br s, 1H); 1.63–1.50 (m, 4H); 1.43–1.30 (m, 4H). ^{13}C NMR (50 MHz, $CDCl_3$) δ (ppm): 155.4; 144.6; 144.5; 143.5; 62.9; 52.9; 49.8; 33.0; 30.2; 27.3; 26.0. HRMS (ESI): m/z calcd for $C_{11}H_{19}N_3ONa$ $[M + Na]^+$: 232.1426; found, 232.1425.

6-((Pyridine-2-ylmethyl)amino)hexan-1-ol (2b). Pyridine-2-carbaldehyde **1b** (0.88 mL, 9 mmol) was added dropwise to 6-aminohexan-1-ol (1.08 g, 9 mmol) dissolved in methanol (20 mL). The mixture was stirred at room temperature in the presence of $MgSO_4$ for 1 h and then filtered. To the filtrate was added sodium borohydride (0.51 g, 14 mmol) in portions at 0 °C. The mixture was stirred at room temperature for 1 h and then, methanol was evaporated. The resulting residue was dissolved in ether (50 mL) and water (50 mL) was added. The aqueous phase was extracted, the organic phase washed with water (2 × 50 mL) and dried with $MgSO_4$. Filtration and evaporation of the solvent made it possible to obtain the product (1.54 g, 82%) as a yellow oil without further purification. ^{1}H NMR (200 MHz, $CDCl_3$) δ (ppm): 8.56 (d, J = 4.5 Hz, 1H); 7.65 (t, J = 7.0 Hz, 1H); 7.30 (d, J = 6.5 Hz, 1H); 7.17 (t, J = 5.0 Hz, 1H); 3.90 (s, 2H); 3.61 (t, J = 5.9 Hz, 2H); 2.66 (t, J = 6.4 Hz, 2H); 2.12 (br s, 1H); 1.67–1.47 (m, 4H); 1.43–1.32 (m, 4H). ^{13}C NMR (50 MHz, $CDCl_3$) δ (ppm): 159.9, 149.7, 137.0, 122.9, 122.5, 63.2, 55.5, 33.1, 30.3, 27.4, 26.0, 18.9. HRMS (ESI): m/z calcd for $C_{12}H_{21}N_2O$ $[M + H]^+$: 209.1654; found, 209.1653.

6-(Benzylamino)hexan-1-ol (2c). Benzaldehyde **1c** (0.87 mL, 9 mmol) was added dropwise to 6-aminohexan-1-ol (1 g, 9 mmol) dissolved in methanol (20 mL). The mixture was stirred at room temperature in the presence of $MgSO_4$ for 1 h and then filtered. To the filtrate was added sodium borohydride (0.48 g, 13 mmol) in portions at 0 °C. The mixture was stirred at room temperature for 1 h and then, methanol was evaporated. The resulting residue was dissolved in ether (50 mL) and water (50 mL) was added. The aqueous phase was extracted, the organic phase washed with water (2 × 50 mL) and dried with $MgSO_4$. Filtration and evaporation of the solvent made it possible to obtain the product (1.72 g, 98%) as a yellow oil without further purification. ^{1}H NMR (200 MHz, $CDCl_3$) δ (ppm): 7.37–7.24 (m, 5H); 3.77 (s, 2H); 3.56 (t, J = 6.5 Hz, 2H); 2.62 (t, J = 6.9 Hz, 2H); 2.52 (br s, 1H); 1.55–1.50 (m, 4H); 1.41–1.25 (m, 4H). ^{13}C NMR (50 MHz, $CDCl_3$) δ (ppm): 140.4; 128.8; 128.6; 127.4; 62.6; 54.4; 49.6; 33.1; 30.3; 27.5; 26.2. HRMS (ESI): m/z calcd for $C_{13}H_{22}NO$ $[M + H]^+$: 208.1701; found, 208.1700.

6-((Thiophen-2-ylmethyl)amino)hexan-1-ol (2d). Thiophene-2-carbaldehyde **1d** (1.24 mL, 13 mmol) was added dropwise to 6-aminohexan-1-ol (1.56 g, 13 mmol) dissolved in methanol (20 mL). The mixture was stirred at room temperature in the presence of $MgSO_4$ for 1 h and then filtered. To the filtrate was added sodium borohydride (0.75 g, 20 mmol) in portions at 0 °C. The mixture was stirred at room temperature for 1 h and then, methanol was evaporated. The resulting residue was

dissolved in ether (50 mL) and water (50 mL) was added. The aqueous phase was extracted, the organic phase washed with water (2 × 50 mL) and dried with $MgSO_4$. Filtration and evaporation of the solvent made it possible to obtain the product (2.43 g, 86%) as a yellow oil without further purification. ^{1}H NMR (200 MHz, $CDCl_3$) δ (ppm): 7.22 (dd, J = 1.6 Hz and 4.8 Hz, 1H); 6.99–6.95 (m, 2H); 4.00 (s, 2H); 3.65 (t, J = 6.7 Hz, 2H); 2.68 (t, J = 7.0 Hz, 2H); 1.62 (br s, 1H); 1.62–1.50 (m, 4H); 1.42–1.36 (m, 4H). ^{13}C NMR (50 MHz, $CDCl_3$) δ (ppm): 144.4; 127.1; 125.4; 124.8; 63.2; 49.4; 48.8; 33.1; 30.3; 27.5; 26.1. HRMS (ESI): m/z calcd for $C_{11}H_{20}NOS$ $[M + H]^+$: 214.1266; found, 214.1266.

General procedure for the synthesis of *N*-tripodal ligands

A mixture of 1-hydroxymethylpyrazole (1.1 eq.) and secondary amine (1 eq.) was stirred without solvent for 3 h at 70 °C. The product was obtained as a yellow oil in quantitative yield in the presence of 10% pyrazole.

6-(((1*H*-Pyrazol-1-yl)methyl)(pyrazin-2-ylmethyl)amino)hexan-1-ol (3a). ^{1}H NMR (200 MHz, $CDCl_3$) δ (ppm): 8.73 (s, 1H); 8.56 (d, J = 2.5 Hz, 1H); 8.50 (d, J = 2.5 Hz, 1H); 7.56 (d, J = 2.0 Hz, 1H); 7.52 (d, J = 2.0 Hz, 1H); 6.33–6.30 (m, 1H); 5.57 (s, 2H); 3.93 (s, 2H); 3.64 (t, J = 6.0 Hz, 2H); 2.62 (t, J = 6.0 Hz, 2H); 1.63–1.51 (m, 4H); 1.38–1.31 (m, 4H). ^{13}C NMR (50 MHz, $CDCl_3$) δ (ppm): 155.2; 145.7; 144.3; 143.6; 140.0; 130.1; 106.0; 69.1; 63.2; 56.3; 52.3; 33.1; 27.8; 27.2; 25.9. HRMS (ESI): m/z calcd for $[C_{15}H_{23}N_5O]^+$: 289.1903; found, 289.1889.

6-(((1*H*-Pyrazol-1-yl)methyl)(pyridin-2-ylmethyl)amino)hexan-1-ol (3b). ^{1}H NMR (200 MHz, $CDCl_3$) δ (ppm): 8.60 (d, J = 5.0 Hz, 1H); 7.71 (m, 1H); 7.57–7.55 (m, 2H); 7.47 (d, J = 7.0 Hz, 1H); 7.22 (m, 1H); 6.32–6.31 (m, 1H); 5.04 (s, 2H); 3.87 (s, 2H); 3.65 (t, J = 6.7 Hz, 2H); 2.62 (t, J = 7.0 Hz, 2H); 1.63–1.53 (m, 4H); 1.40–1.33 (m, 4H). ^{13}C NMR (50 MHz, $CDCl_3$) δ (ppm): 159.6; 149.7; 139.6; 137.0; 130.5; 123.6; 122.6; 105.8; 69.1; 63.1; 58.3; 52.3; 33.1; 27.8; 27.3; 25.9. HRMS (ESI): m/z calcd for $C_{16}H_{24}N_4ONa$ $[M + Na]^+$: 311.1848; found, 311.1845.

6-(((1*H*-Pyrazol-1-yl)methyl)(benzyl)amino)hexan-1-ol (3c). ^{1}H NMR (200 MHz, $CDCl_3$) δ (ppm): 7.56–7.55 (m, 1H); 7.45–7.25 (m, 6H); 6.34–6.26 (m, 1H); 4.97 (s, 2H); 3.69 (s, 2H); 3.62 (t, J = 6.8 Hz, 2H); 2.58 (t, J = 7.0 Hz, 2H); 2.05 (br s, 1H); 1.65–1.46 (m, 4H); 1.42–1.25 (m, 4H). ^{13}C NMR (50 MHz, $CDCl_3$) δ (ppm): 139.6; 139.3; 130.3; 129.1; 128.8; 127.6; 105.6; 68.7; 63.2; 56.4; 51.9; 33.1; 27.8; 27.3; 25.9. HRMS (ESI): m/z calcd for $C_{17}H_{25}N_3ONa$ $[M + Na]^+$: 310.1895; found, 310.1896.

6-(((1*H*-Pyrazol-1-yl)methyl)(thiophen-2-ylmethyl)amino)hexan-1-ol (3d). ^{1}H NMR (200 MHz, $CDCl_3$) δ (ppm): 7.55 (d, J = 2.5 Hz, 1H); 7.44 (d, J = 2.5 Hz, 1H); 7.28–7.27 (m, 1H); 6.98–6.97 (m, 2H); 6.32–6.30 (m, 1H); 5.01 (s, 2H); 3.89 (s, 2H); 3.65 (t, J = 6.7 Hz, 2H); 2.61 (t, J = 7.0 Hz, 2H); 1.63–1.53 (m, 4H); 1.40–1.33 (m, 4H). ^{13}C NMR (50 MHz, $CDCl_3$) δ (ppm): 143.4; 139.7; 130.4; 127.0; 126.3; 125.5; 105.8; 68.4; 63.2; 51.7; 51.2; 33.1; 27.8; 27.2; 25.9. HRMS (ESI): m/z calcd for $C_{15}H_{23}N_3ONaS$ $[M + Na]^+$: 316.1459; found, 316.1462.

General procedure for the synthesis of monocopper complexes. Copper(II) chloride (1 eq.) and *N*-tripodal ligand (1.2 eq.) were stirred in anhydrous THF for 2 h at room temperature. A solid was formed or the complex was precipitated by addition of anhydrous ether or dichloromethane. The precipitate was filtered under argon, washed with ether or dichloromethane and dried under vacuum. The anhydrous complex was then dissolved in MeOH : H_2O (95 : 5) and the solvent was evaporated under reduced pressure to obtain the hydrated form of the complex.

4a. Yield 57% of a blue-green powder. HRMS (ESI): m/z calcd for $C_{15}H_{23}ClCuN_5O$ $[M - Cl]^+$: 387.0887; found, 387.0887.

4b. Yield 52% of a blue powder. HRMS (ESI): m/z calcd for $C_{16}H_{24}ClCuN_4O$ $[M - Cl]^+$: 386.0934; found, 386.0933.

4c. Yield 55% of a green powder. HRMS (ESI): m/z calcd for $C_{17}H_{25}ClCuN_3O$ $[M - Cl]^+$: 385.0982; found, 385.0981.

4d. Yield 61% of a green powder. Found, C, 39.91; H, 5.92; N, 9.37; S, 7.06%. Calc. for $C_{15}H_{25}N_3O_2Cl_2SCu$: C, 40.40; H, 5.65; N, 9.42; S, 7.19%.

Catalysis

The experiments were conducted in air at constant stirring and temperature of 25 °C, monitored with a contact thermomether dipped in the solution. 6 mL of a 10^{-4} mol L^{-1} solution of copper complex in methanol was added under stirring to a fresh solution of 10^{-2} mol L^{-1} of 3,5-di-*tert*-butylcatechol in 40 mL methanol maintained at 25 °C. The absorbance was continually monitored at 400 nm for 1 h using a dipping probe colorimeter (662 photometer from Metrohm) to detect the *o*-quinone characteristic signal.

Notes and references

1 T. Klabunde, C. Eicken, J. C. Sacchettini and B. Krebs, *Nat. Struct. Biol.*, 1998, **5**, 1084.
2 W. T. Ismaya, H. J. Rozeboom, A. Weijn, J. J. Mes, F. Fusetti, H. J. Wichers and B. W. Dijkstra, *Biochemistry*, 2011, **50**, 5477.
3 H. Decker, T. Schweikardt and F. Tuczek, *Angew. Chem., Int. Ed.*, 2006, **45**, 4546.
4 S. Halaouli, M. Asther, J. C. Sigoillot, M. Hamdi and A. Lomascolo, *J. Appl. Microbiol.*, 2006, **100**, 219.
5 S. Y. Lee, B. L. Lee and K. Soderhall, *Biochem. Biophys. Res. Commun.*, 2004, **322**, 490.
6 K. Lerch, C. Longoni and E. Jordi, *J. Biol. Chem.*, 1982, **257**, 6408.
7 H. Claus and H. Decker, *Syst. Appl. Microbiol.*, 2006, **29**, 3.
8 J. C. Garcia-Borron and F. Solano, *Pigm. Cell Res.*, 2002, **15**, 162.
9 C. Gielens, K. Idakieva, M. De Maeyer, V. Van den Bergh, N. I. Siddiqui and F. Compernolle, *Peptides*, 2007, **28**, 790.
10 K. S. Banu, T. Chattopadhyay, A. Banerjee, S. Bhattacharya, E. Zangrando and D. Das, *J. Mol. Catal. A: Chem.*, 2009, **310**, 34.
11 K. S. Banu, T. Chattopadhyay, A. Banerjee, S. Bhattacharya, E. Suresh, M. Nethaji, E. Zangrando and D. Das, *Inorg. Chem.*, 2008, **47**, 7083.
12 M. Gullotti, L. Santagostini, R. Pagliarin, A. Granata and L. Casella, *J. Mol. Catal. A: Chem.*, 2005, **235**, 271.
13 J. Mukherjee and R. Mukherjee, *Inorg. Chim. Acta*, 2002, **337**, 429.
14 S. Torelli, C. Belle, S. Hamman, J. L. Pierre and E. Saint-Aman, *Inorg. Chem.*, 2002, **41**, 3983.
15 A. Neves, L. M. Rossi, A. J. Bortoluzzi, B. Szpoganicz, C. Wiezbicki and E. Schwingel, *Inorg. Chem.*, 2002, **41**, 1788.
16 S. Anbu, M. Kandaswamy, P. Suthakaran, V. Murugan and B. Varghese, *J. Inorg. Biochem.*, 2009, **103**, 401.
17 R. A. Peralta, A. Neves, A. J. Bortoluzzi, A. dos Anjos, F. R. Xavier, B. Szpoganicz, H. Terenzi, M. C. B. de Oliveira,

E. Castellano, G. R. Friedermann, A. S. Mangrich and M. A. Novak, *J. Inorg. Biochem.*, 2006, **100**, 992.
18 P. Kamatchi, S. Selvaraj and M. Kandaswamy, *Polyhedron*, 2005, **24**, 900.
19 M. Merkel, N. Möller, M. Piacenza, S. Grimme, A. Rompel and B. Krebs, *Chem.–Eur. J.*, 2005, **11**, 1201.
20 C. Fernandes, A. Neves, A. J. Bortoluzzi, A. S. Mangrich, E. Rentschler, B. Szpoganicz and E. Schwingel, *Inorg. Chim. Acta*, 2001, **320**, 12.
21 A. Neves, L. M. Rossi, A. Horn, I. Vencato, A. J. Bortoluzzi, C. Zucco and A. S. Mangrich, *Inorg. Chem. Commun.*, 1999, **2**, 334.
22 E. V. RybakAkimova, D. H. Busch, P. K. Kahol, N. Pinto, N. W. Alcock and H. J. Clase, *Inorg. Chem.*, 1997, **36**, 510.
23 M. Lubben, R. Hage, A. Meetsma, K. Byma and B. L. Feringa, *Inorg. Chem.*, 1995, **34**, 2217.
24 I. A. Koval, M. Huisman, A. F. Stassen, P. Gamez, O. Roubeau, C. Belle, J. L. Pierre, E. Saint-Aman, M. Lüken, B. Krebs, M. Lutz, A. L. Spek and J. Reedijk, *Eur. J. Inorg. Chem.*, 2004, 4036.
25 M. Huisman, I. A. Koval, P. Gamez and J. Reedijk, *Inorg. Chim. Acta*, 2006, **359**, 1786.
26 Y. F. F. Song, C. Massera, M. Quesada, I. A. Koval, P. Gamez, A. M. M. Lanfredi and J. Reedijk, *Eur. J. Inorg. Chem.*, 2004, 4566.
27 V. K. Bhardwaj, N. Aliaga-Alcalde, M. Corbella and G. Hundal, *Inorg. Chim. Acta*, 2010, **363**, 97.
28 A. Kupan, J. Kaizer, G. Speier, M. Giorgi, M. Reglier and F. Pollreisz, *J. Inorg. Biochem.*, 2009, **103**, 389.
29 M. El Kodadi, F. Malek, R. Touzani and A. Ramdani, *Catal. Commun.*, 2008, **9**, 966.
30 I. Bouabdallah, R. Touzani, I. Zidane and A. Ramdani, *Catal. Commun.*, 2007, **8**, 707.
31 A. Panja, S. Goswami, N. Shaikh, P. Roy, M. Manassero, R. J. Butcher and P. Banerjee, *Polyhedron*, 2005, **24**, 2921.
32 P. S. Subramanian, E. Suresh and R. S. Shukla, *Inorg. Chim. Acta*, 2005, **358**, 2651.
33 Z. F. Chen, Z. R. Liao, D. F. Li, W. K. Li and X. G. Meng, *J. Inorg. Biochem.*, 2004, **98**, 1315.
34 Y. T. Cheng, H. L. Chen, S. Y. Tsai, C. C. Su, H. S. Tsang, T. S. Kuo, Y. C. Tsai, F. L. Liao and S. L. Wang, *Eur. J. Inorg. Chem.*, 2004, 2180.
35 G. T. Musie, X. B. Li and D. R. Powell, *Inorg. Chim. Acta*, 2003, **348**, 69.
36 M. Gupta, P. Mathur and R. J. Butcher, *Inorg. Chem.*, 2001, **40**, 878.
37 M. R. Malachowski, J. Carden, M. G. Davidson, W. L. Driessen and J. Reedijk, *Inorg. Chim. Acta*, 1997, **257**, 59.
38 M. R. Malachowski, B. Dorsey, J. G. Sackett, R. S. Kelly, A. L. Ferko and R. N. Hardin, *Inorg. Chim. Acta*, 1996, **249**, 85.
39 M. R. Malachowski, H. B. Huynh, L. J. Tomlinson, R. S. Kelly and J. W. F. Jun, *J. Chem. Soc., Dalton Trans.*, 1995, 31.
40 M. R. Malachowski, L. J. Tomlinson, M. G. Davidson and M. J. Hall, *J. Coord. Chem.*, 1992, **25**, 171.
41 M. R. Malachowski, M. E. Adams, D. Murray, R. White, N. Elia, A. L. Rheingold, L. N. Zakharov and R. S. Kelly, *Inorg. Chim. Acta*, 2009, **362**, 1247.
42 M. R. Malachowski, M. Adams, N. Elia, A. L. Rheingold and R. S. Kelly, *J. Chem. Soc., Dalton Trans.*, 1999, 2177.
43 R. Marion, M. Zaarour, N. A. Qachachi, N. M. Saleh, F. Justaud, D. Floner, O. Lavastre and F. Geneste, *J. Biol. Inorg. Chem.*, 2011, **105**, 1391.
44 R. Marion, G. Muthusamy and F. Geneste, *J. Catal.*, 2012, **286**, 266.
45 B. J. Hathaway and D. E. Billing, *Coord. Chem. Rev.*, 1970, **5**, 143.
46 J. Peisach and W. E. Blumberg, *Arch. Biochem. Biophys.*, 1974, **165**, 691.
47 A. Bencini, I. Bertini, D. Gatteschi and A. Scozzafava, *Inorg. Chem.*, 1978, **17**, 3194.
48 M. El Kodadi, M. Fouad, A. Ramdani, D. Eddike, M. Tillard and C. Belin, *Acta Cryst.*, 2004, **E60**, m426.
49 R. Touzani, S. Garbacia, O. Lavastre, V. K. Yadav and B. Carboni, *J. Comb. Chem.*, 2003, **5**, 375.
50 I. A. Koval, P. Gamez, C. Belle, K. Selmeczi and J. Reedijk, *Chem. Soc. Rev.*, 2006, **35**, 814.
51 M. Kodera, T. Kawata, K. Kano, Y. Tachi, S. Itoh and S. Kojo, *Bull. Chem. Soc. Jpn.*, 2003, **76**, 1957.
52 I. Dvoretzky and G. H. Richter, *J. Org. Chem.*, 1950, **15**, 1285.
53 O. Branytska, L. J. W. Shimon and R. Neumann, *Chem. Commun.*, 2007, 3957.